Molecular Immunology xxx (2015) xxx–xxx

Contents lists available at ScienceDirect

Molecular Immunology

journal homepage: www.elsevier.com/locate/molimm

Effects of polymorphic variation on the mechanism of Endoplasmic Reticulum Aminopeptidase 1

Athanasios Stamogiannos, Despoina Koumantou, Athanasios Papakyriakou**, Efstratios Stratikos*

National Center for Scientific Research Demokritos, Agia Paraskevi, Athens 15310, Greece

ARTICLE INFO

Article history:
Received 21 May 2015
Received in revised form 1 July 2015
Accepted 8 July 2015
Available online xxx

Keywords:
Antigen processing
Antigen epitopes
Peptides
Aminopeptidase
Accelerated molecular dynamics
Principle component analysis
Single nucleotide polymorphisms (SNPs)

ABSTRACT

Endoplasmic Reticulum Aminopeptidase 1 (ERAP1) generates antigenic peptides for loading onto Major Histocompatibility Class I molecules (MHCI) and can regulate adaptive immune responses. During the last few years, many genetic studies have revealed strong associations between coding Single Nucleotide Polymorphisms (SNPs) in ERAP1 and common human diseases ranging from viral infections to cancer and autoimmunity. Functional studies have established that these SNPs affect enzyme activity resulting to changes in antigenic peptide processing, presentation by MHCI and cellular cytotoxic responses. These disease-associated polymorphisms are, however, located away from the enzyme's active site and are interspersed to different structural domains. As a result, the mechanism by which these SNPs can affect function remains largely elusive. ERAP1 utilizes a complex catalytic mechanism that involves a large conformational change between inactive and active forms and has the unique property to trim larger peptides more efficiently than smaller ones. We analyzed two of the most consistently discovered disease-associated polymorphisms, namely K528R and Q730E, for their effect on the ability of the enzyme to select substrates based on length and to undergo conformational changes. By utilizing enzymatic and computational analysis we propose that disease-associated SNPs can affect ERAP1 function by influencing: (i) substrate length selection and (ii) the conformational distribution of the protein ensemble. Our results provide novel insight on the mechanisms by which polymorphic variation distal from the active site of ERAP1 can translate to changes in function and contribute to immune system variability in humans.

1. Introduction

Cytotoxic T-lymphocyte (CTL) responses towards infected or aberrant cells are central to the ability of the adaptive immune response to fight pathogens. CTLs recognize infected cells by means of specific antigenic peptides bound onto specialized receptors of the Major Histocompatibility class I (MHCI) on the surface of all somatic cells. These antigenic peptides are derived from the proteolytic digestion of intracellular proteins and represent a sample of the protein content of the cell (Lazaro et al., 2015). Recognition of antigenic peptides that do not belong to the normal protein content of the cell indicates infection or malignant transformation, eliciting specific cytotoxic responses that eradicate the cell (Weimershaus et al., 2013).

During the last decade the trimming of N-terminal extended precursor peptides by ER-resident aminopeptidase ERAP1 has been recognized to be key for the generation of antigenic peptides (Weimershaus et al., 2013; Evnouchidou et al., 2009). ERAP1 is necessary for the generation of many antigenic epitopes but can also over-trim others, leading to their destruction (Blanchard and Shastri, 2008). It is a 110 kDa zinc-aminopeptidase that belongs to the M1 family of metallopeptidases, but has several unique properties that fit well with its biological role. First, it can efficiently process many different peptide substrates, consistent with the vast variety of peptide sequences that it may encounter in the ER. Secondly, it prefers to trim larger peptides over smaller ones, resulting to the accumulation of products of 8-9 amino acids long, a length consistent with the binding preferences of MHCI (Chang et al., 2005). Lastly, ERAP1 activity can be dependent on the whole peptide sequence, a property that can affect the pool of antigenic peptides available for MHCI presentation (Evnouchidou et al., 2008).

Crystallographic and biochemical analysis of ERAP1 has revealed that during its catalytic cycle the enzyme can undergo a signif-

* Corresponding author: Fax: +30 2106503918.
** Corresponding author.
E-mail addresses: thpap@rrp.demokritos.gr (A. Papakyriakou), stratos@rrp.demokritos.gr (E. Stratikos).

http://dx.doi.org/10.1016/j.molimm.2015.07.010
0161-5890/

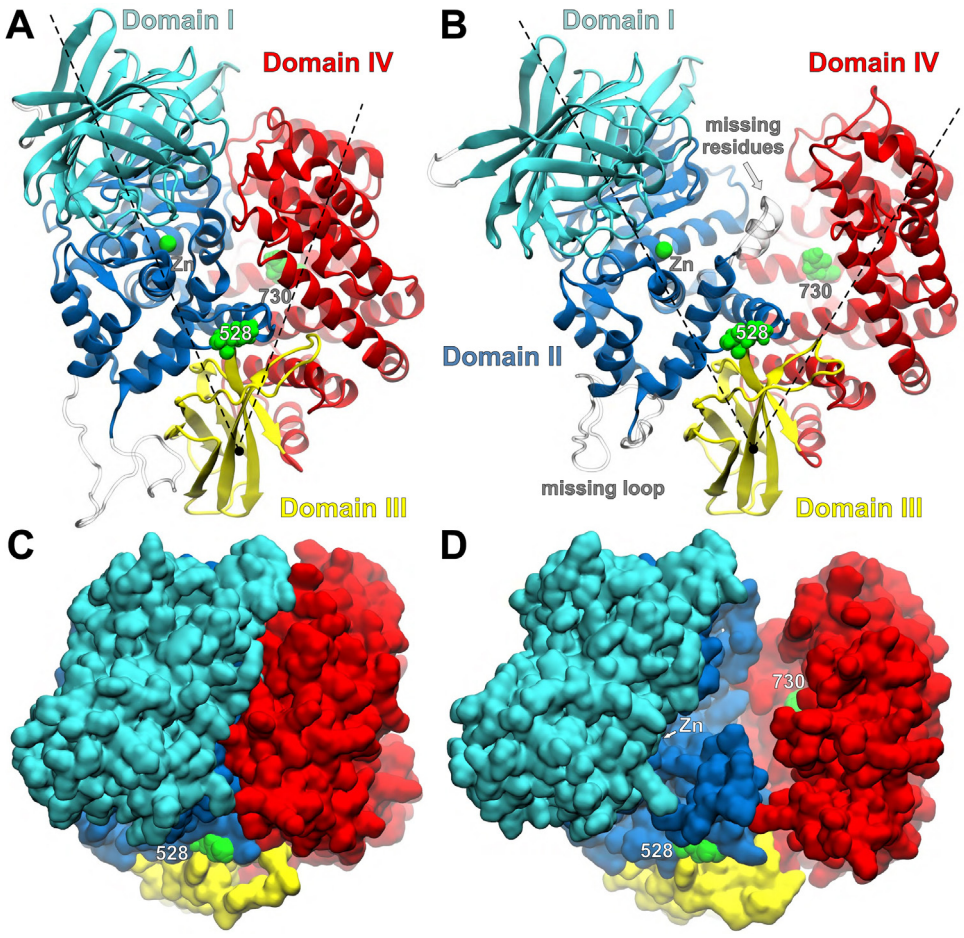

Fig. 1. Crystallographic structures of ERAP1 in the closed (A, PDB: 2YD0) and open states (B, PDB: 3MDJ), illustrating the domain organization of the enzyme, the catalytic Zn and the polymorphic residues at positions 528 and 730. The missing residues (417–433) in the open state, and the missing loop (486–514) in both X-ray structures were modeled and are shown in gray. The interdomain angle theta is defined using the centers of mass of domains I and II (excluding the missing loop), domain III and domain IV, and is 53° in the closed and 67° in the open state. (C and D) Surface representation of the two ERAP1 states from the top of the substrate binding site indicating the position of the two polymorphic residues.

icant conformational change that involves reorganization of key structural domains of the enzyme from an open to a closed state (reviewed in (Stratikos and Stern, 2013)). An extended internal cavity hypothesized to accommodate the peptide-substrate is only exposed to the external solvent in the open conformation (Fig. 1). Therefore, the open state has been suggested to facilitate initial substrate capture and the closed state to enhance catalysis by organizing catalytic residues and specificity pockets. Larger peptides may facilitate this transition through a mechanism of self-activation involving a still unmapped regulatory site in the enzyme (Nguyen et al., 2011; Gandhi et al., 2011; Kochan et al., 2011). Overall, it appears that ERAP1 has evolved to specialize for generating antigenic peptides for MHCI.

Several population genetic studies have associated several coding single nucleotide polymorphisms (SNPs) in ERAP1 with predisposition to major human diseases ranging from viral infections to cancer and autoimmunity (reviewed in (Fruci et al., 2014; Alvarez-Navarro and Lopez de Castro, 2014)). These associations have been repeatedly confirmed especially for autoimmune diseases often in the context of specific MHCI alleles, suggesting that the disease-link lies within the role of ERAP1 in generating antigenic peptides (Alvarez-Navarro and Lopez de Castro, 2014; The Australo-Anglo-American Spondyloarthritis et al., 2011). Several studies have also demonstrated that these disease-associated variants affect ERAP1 enzymatic activity and selectivity, cellular antigen presentation and concomitant cytotoxic responses (Evnouchidou et al., 2011; Chen et al., 2014; Reeves et al., 2013; Garcia-Medel et al., 2012; Sanz-Bravo et al., 2015; Alvarez-Navarro et al., 2015; Martin-Esteban et al., 2014). Interestingly, in several of those studies, changes in ERAP1 activity due to polymorphic variation at positions 528 and 730 have been correlated with the production of different lengths of antigenic peptides although the effects of peptide sequence were not investigated in those studies (Garcia-Medel et al., 2012; Sanz-Bravo et al., 2015; Alvarez-Navarro et al., 2015). Specific ERAP1 haplotypes have been proposed to constitute a range of different activities that correlate to disease predisposition (Reeves et al., 2013; Seregin et al., 2013). This association is reminiscent of the natural variability in MHCI molecules: polymorphisms in the MHC locus define thousands of MHCI alleles within the population and affect antigenic peptide binding and presentation as well as resulting adaptive immune responses to pathogens. Most polymorphisms in MHCI cluster within and around the peptide binding pocket, directly affecting peptide binding or interactions with the T-cell receptor (Reche and Reinherz, 2003). In contrast, most disease-associated polymorphisms in ERAP1 are located distal to the active site and are scattered to different structural domains (Nguyen et al., 2011). As a result, little insight exists on how a diverse set of natural polymorphisms dispersed over the struc-

Please cite this article in press as: Stamogiannos, A., et al., Effects of polymorphic variation on the mechanism of Endoplasmic Reticulum Aminopeptidase 1. Mol. Immunol. (2015), http://dx.doi.org/10.1016/j.molimm.2015.07.010

ture of this enzyme can affect function and predisposition to disease.

In this study, we employed a combination of experimental and computational approaches in order to address the lack of mechanistic insight on how ERAP1 SNPs affect enzyme function. We focused our analysis on two common ERAP1 SNPs, K528R, and Q730E that have been consistently discovered to associate with disease predisposition and to affect antigen presentation in cells. Furthermore, these two polymorphisms are distinct in being located inside and outside the central cavity of ERAP1 and are therefore likely to affect activity by different mechanisms. We first examined if polymorphic variation in ERAP1 can affect peptide length selection using a collection of polyglycine peptides of increasing length to isolate length-dependent effects from sequence-dependent effects. We also employed molecular dynamics calculations to analyze the conformational rearrangements of ERAP1 and how these rearrangements are affected by polymorphic variation. Our analysis points to two distinct but complementary molecular mechanisms that contribute to the effects of SNPs to ERAP1 function.

2. Materials and methods

2.1. Peptides

All peptides were purchased from JPT peptide technologies GmbH (Berlin, Germany) and purified by reverse-phase HPLC (chromolith C-18 column, Merck) to >95% purity.

2.2. Protein expression and purification

The generation of ERAP1 variants with C-terminal His tags in the pDEST8 vector (Invitrogen) has been described elsewhere (Goto et al., 2006). The baculovirus expression system (Invitrogen) was used for the expression of ERAP1 variants. Briefly, competent DH10bac *Escherichia coli* cells were transformed with the pDEST8 vectors containing ERAP1 alleles. These cells harbor a plasmid that contains the baculovirus genome (bacmid) and a transposition helper vector. The recombinant bacmid DNA was isolated and used to transfect insect Sf9 cells using the Cellfectin reagent (Invitrogen). After a 3-day incubation period the baculovirus was harvested from the cell supernatant. Larger amounts of virus were produced by infecting Hi5 cells grown in suspension and collecting the supernatant 3–7 days post infection. Hi5 insect cells grown in sf900II serum-free medium (Invitrogen), were infected with baculoviruses carrying ERAP1 alleles and 3–4 days later the cell medium, that contained the secreted enzyme, was harvested by centrifugation. The cell supernatant was extensively dialyzed against a 10 mM phosphate buffer pH 8.0, containing 100 mM NaCl. After the dialysis, the supernatant composition was adjusted to 50 mM sodium phosphate pH 8.0, 300 mM sodium chloride and 10 mM imidazole and then mixed with Ni-NTA resin and allowed to bind with mild stirring for 1hr. The slurry was packed to a gravity column and washed. The protein was eluted using a 20–150 mM imidazole step-gradient. The fractions collected were tested for aminopeptidase enzymatic activity, using L-leucine 7-amido-4-methyl coumarin (L-AMC) as substrate and the enzyme purity was validated with SDS-PAGE. The ERAP1-containing fractions were dialyzed against a 10 mM Hepes pH 7.0, 100 mM NaCl buffer and stored as single use aliquots with 10% glycerol at −80 °C. The proteins were quantified by SDS-PAGE densitometry, using ImageJ software and known concentration ERAP1 standards.

2.3. Enzymatic assays

The aminopeptidase activity of the recombinant ERAP1 was followed during the expression and purification steps by the fluorescent signal produced upon digestion of the substrate L-AMC (Sigma–Aldrich). The fluorescence was measured at 460 nm, while the excitation was set at 380 nm. All measurements were performed on a TECAN infinite M200 microplate fluorescence reader. The activity of ERAP1 alleles was compared using the same assay.

For analysis of the digestion of the LG_XL peptides, 20 μM of peptide was incubated with 10 nM or 100 nM of ERAP1, at 37 °C for 1 h, in a 50 mM Hepes pH 7.0, 100 mM NaCl buffer. Reactions were terminated with the addition of 0.25% (v/v) trifluoroacetic acid (TFA). The reactions were analyzed in a reverse phase-HPLC (chromolith C-18 column, Merck) by following the absorbance at 220 nm. A linear gradient elution system was used (solvent A: 0.05% TFA, solvent B: 0.05% TFA, 40% ACN). The percentage of the substrate cleaved was calculated by integration of the area under each peptide peak, using appropriate standards. Specific activity was calculated using the GraphPad software, by fitting the results in a one phase decay equation: $Y = Y_0 \times e^{(-k \times x)}$, where x is the reaction time, Y_0 the substrate fraction left intact after $t = 0$ s (constrained as $Y = 1$), Y the substrate fraction left intact after the end of the reaction and k the reaction rate constant.

2.4. Computational methods

2.4.1. Preparation of the simulation systems

The initial models were based on the X-ray crystal structures of human ERAP1 complexes with bestatin, either in the closed state (PDB ID: 2YD0) (Kochan et al., 2011) or the open states (PDB ID: 3MDJ) (Nguyen et al., 2011). Protein residues 46–934 and the zinc ion were used for the simulations of ligand-free ERAP1. For the closed state, the alternative location–A atoms of residues D284, C736, C743, and H873 were retained. The missing residues 111–114, 486–513, and 553–557 were added using MODELLER (v9.10) (Fiser and Sali, 2003). The lowest DOPE score (Shen and Sali, 2006) model was selected from 30 runs for further refinement of the missing loop 486–513 using the automatic loop refinement method. The protonation state of histidine residues was set after calculation of their pK values using H++ (v3.1) (Anandakrishnan et al., 2012) and visual inspection of their neighboring residues for putative hydrogen bonding interactions. In particular, the two zinc-bound H353 and H357, along with H468, H501, H511, and H738 were set to be protonated at $H^{\delta 1}$, whereas, all the remaining histidine residues were protonated at $H^{\epsilon 2}$. For the initial open state of ERAP1, we selected chain C of PDB ID 3MDJ that displays the larger interdomain angle among the 3 conformations found in the asymmetric unit. The natural variant residues D346, R528 and E730 were changed to G346, K528 and Q730 on the basis of UniProt entry Q9NZ08 for the modeling of the ancestral protein (ERAP1-KQ), as in the closed ERAP1. The missing residues 111–112 were taken from chain B, while residues 417–433, 864–867, 893–906 were modeled using the corresponding residues that were resolved in the closed ERAP1 structure after superimposing the adjacent residues. The missing loop residues 486–514 and 552–555 were modeled using MODELER as described for the closed ERAP1. The simulation systems were prepared using the LEaP module of AMBER (v12) package (Case et al., 2005). Specifically, hydrogen atoms were added, two disulfide bonds were formed between C404–C443 and C736–C743, and a water molecule was added to fill the tetrahedral coordination sphere of the catalytic zinc. The ff12SB parameters (Hornak et al., 2006) were applied to the protein atoms and a simple bonded model was employed for zinc (Papakyriakou et al., 2007). The protein was solvated in a box of 32,525 TIP3P (Jorgensen et al., 1983) water molecules and then 119 Na^+ and 105 Cl^- ions were added to neutralize the systems and simulate an ionic strength of 0.15 M. The simulation systems of the nat-

Please cite this article in press as: Stamogiannos, A., et al., Effects of polymorphic variation on the mechanism of Endoplasmic Reticulum Aminopeptidase 1. Mol. Immunol. (2015), http://dx.doi.org/10.1016/j.molimm.2015.07.010

ural variants K528R (ERAP1-RQ) and Q730E (ERAP1-KE) in the open and closed states were prepared from the models of the ancestral ERAP1-KQ by changing the corresponding residue only (Fig. 1).

2.4.2. Conventional and accelerated molecular dynamics simulations

Conventional (cMD) and accelerated (aMD) molecular dynamics simulations were performed with the GPU-version of PMEMD program using periodic boundary conditions (Salomon-Ferrer et al., 2013). A time step of 2.0 fs was used and the SHAKE algorithm (Ryckaert et al., 1977) was employed to constrain the bonds connecting hydrogen atoms. The temperature was controlled using a Langevin thermostat (Pastor et al., 1988) with a collision frequency of 2.0 ps^{-1}, and the pressure was regulated at 1 bar using the Berendsen weak-coupling algorithm (Berendsen et al., 1984) with a relaxation time of 2.0 ps. Electrostatic interactions were evaluated by means of the Particle Mesh Ewald method (Darden et al., 1993) with a real space cutoff of 9.0 Å and a direct sum tolerance of 10^{-6}. The translational center-of-mass motion was removed every 2.0 ps.

Each system was initially minimized to remove any close contacts and then harmonic positional restraints of 10 Kcal mol^{-1} $Å^{-2}$ force constant were applied to the protein backbone atoms. The temperature was increased from 10 K to 300 K as a linear function of time over the course of 300 ps. The restraints were then removed over 4 rounds of 50-ps in the isotherman–isobaric (NPT) ensemble by reducing their strength (5.0, 2.0, 1.0, 0.5 Kcal mol^{-1} $Å^{-2}$) and an additional 9.5 ns at constant isotropic pressure and temperature of 300 K was carried out. Production runs of 100 ns were performed in the isothermal–isovolumetric (NVT) under the same conditions as described above, and snapshots were collected every 1000 steps.

To enhance exploration of the conformational space, five independent aMD calculations of 50×10^6 steps (100 ns each) were seeded from the three open ERAP1 cMD at 30, 50, 70, 90 and 110 ns. An average total potential energy and average torsional potential energy was computed from the last 50 ns cMD and used for the dual boost potential of the aMD. Selection of the boost parameters was based on previous work by the McCammon group (Hamelberg et al., 2004, 2007). In particular, the total boost parameter α_{tot} was set equal to 0.16 Kcal mol^{-1} $atom^{-1}$ × (total number of atoms), and the torsional boost parameter α_{tor} equal to (1/5) (4 Kcal mol^{-1} $residue^{-1}$ × (number of solute residues). For the closed ERAP1 states, we performed 2 rounds of 25×10^6 aMD steps with one normal, and one higher-acceleration round increasing the torsional boost potential threshold by α_{tor}. The number of aMD simulation steps is used since the timescale of aMD is non-linear and cannot be assessed accurately. The bias potentials were collected every 1000 steps for both total and torsional boost, and then each frame was reweighted based on a Maclaurin series expansion to the 10^{th} order using the PyReweighting Python scripts (Miao et al., 2014).

Principal component and trajectory analysis was performed with the CPPTRAJ module of AmberTools (v13) (Roe and Cheatham, 2013) after mass-weighted RMSD fitting with respect to domain III (residues 530–614) of the closed ERAP1-KQ state, while excluding the flexible loop residues 486–514. The interdomain angle is defined as the angle of the centers of mass of domains I and II (46–529), domain III (530–614) and domain IV (615–940), excluding the missing loop (486–514). Visual inspection of the trajectories and rendering of the figures was performed with VMD (v1.9) (Humphrey et al., 1996). Calculations were performed on Intel workstations equipped with NVIDIA GTX 780 GPUs and running Linux x86_64 kernel v2.6.32.

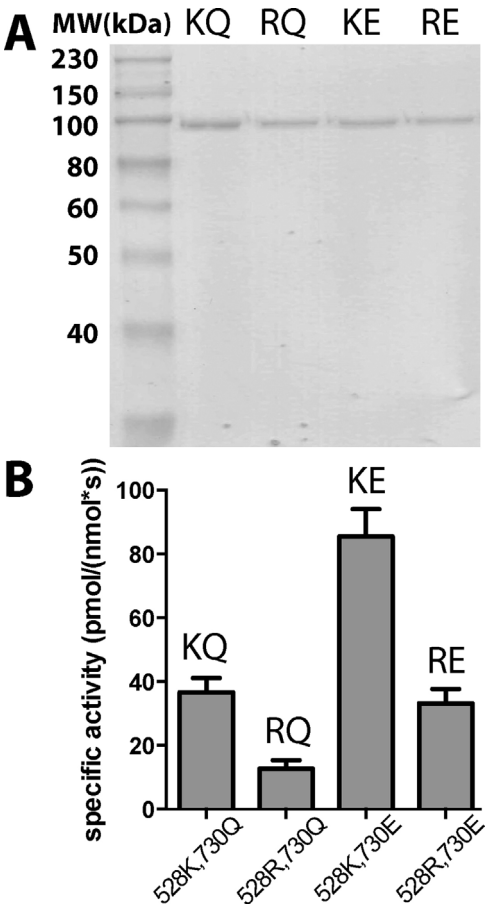

Fig. 2. (A) SDS-PAGE analysis of four variants of ERAP1 carrying all possible combinations of the common polymorphisms at positions 528 and 730. The variants are presented in the picture in the same order as in panel B. (B), specific activities of the four ERAP1 variants towards hydrolysis of the fluorigenic substrate Leu-AMC.

3. Results

3.1. ERAP1 SNPs affect enzymatic activity against model fluorigenic substrates

To study the functional effects of ERAP1 SNPs we constructed four ERAP1 alleles that vary in positions 528 and 730, two positions consistently discovered in population studies to associate with predisposition to autoimmunity in an HLA-specific fashion, and which been demonstrated to affect antigen presentation in multiple assays. Our control allele, which corresponds to the combination of ancestral SNPs 528K, and 730Q (henceforth named allele KQ), was used to generate two single substitution alleles 528R, 730Q, and 528K, 730E (alleles RQ and KE, respectively), as well as the double-substituted 528R, 730E (allele RE). These two positions are distal to the enzyme's active site (by 23 Å and 30 Å, respectively, see Fig. 1) and are localized at the beginning of domain III (position 528) and at domain IV of the enzyme (position 730). Each allele was produced in recombinant form, purified and used for enzymatic assays (Fig. 2A). All four alleles were found to be enzymatically active against small fluorigenic substrates (Fig. 2B). However, we found statistically significant differences between alleles that were consistent between protein preparations and largely in agreement with published literature. For example, the 528R polymorphism led to an enzyme that had a specific activity of about 50% compared to the control enzyme, consistent with previous analyses (Garcia-Medel et al., 2012; Goto et al., 2006; Evans et al., 2011). The effects of the polymorphic variation to enzyme activity appeared to

Please cite this article in press as: Stamogiannos, A., et al., Effects of polymorphic variation on the mechanism of Endoplasmic Reticulum Aminopeptidase 1. Mol. Immunol. (2015), http://dx.doi.org/10.1016/j.molimm.2015.07.010

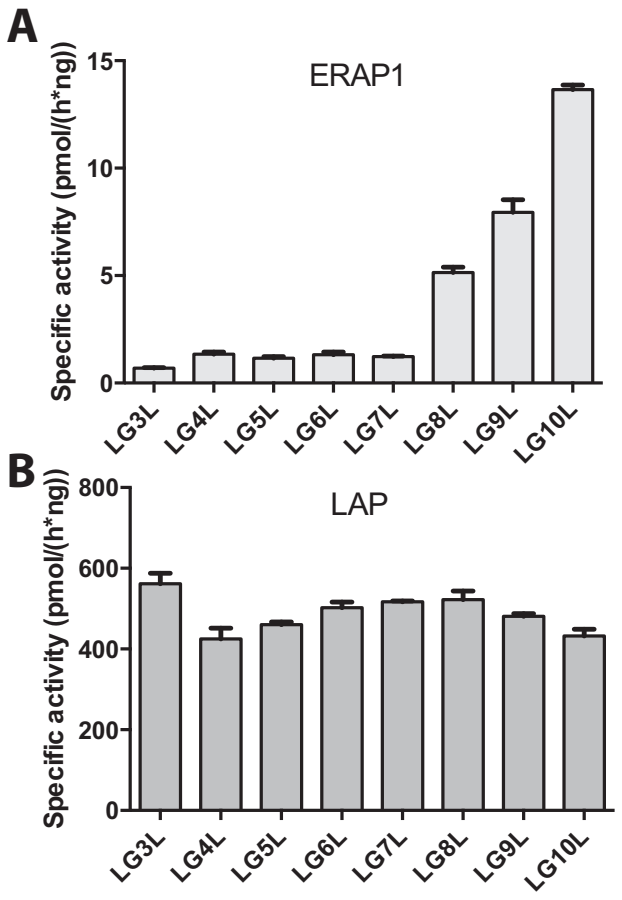

Fig. 3. Comparison of length selection by ERAP1 and LAP. (A) Specific activity of ERAP1 towards the hydrolysis of the N-terminal leucine residue of poly-glycine containing peptides, followed by HPLC. (B) Specific activity of LAP towards the hydrolysis of the same peptide series.

also be additive: the K528R substitution led to a less active enzyme and the Q730E substitution to a more active enzyme, whereas the combination of changes almost canceled each other out (Fig. 2B).

3.2. ERAP1 shows selectivity for larger peptides

It has been suggested that ERAP1 is specialized for the trimming of peptides longer than 9 amino acids, consistent with its role in preparing antigenic epitopes of 8-9 amino acid long from extended precursors (Chang et al., 2005; Evnouchidou et al., 2008; Nguyen et al., 2011). Using our recombinant ERAP1 alleles, we tested their ability to trim a collection of poly-glycine containing peptides of the sequence LG_xL where x varies from 3 to 10 glycine residues. These peptides were designed to carry a near-optimal N-terminal residue for ERAP1, as well as the same C-terminal residue that has been proposed to be important for trimming (Chang et al., 2005). The rest of the peptide sequence consists of glycine residues that lack side chains, in order to isolate length-dependent effects by eliminating any possible interactions with putative specificity pockets along the peptide binding cavity (Evnouchidou et al., 2008). Trimming of the N-terminal leucine residue by ERAP1 was faster for larger peptides of >10 residues long, consistent with the length selection properties of ERAP1 (Fig. 3). In contrast, trimming by the cytosolic Leucine-aminopeptidase (LAP), a metabolic enzyme not essential for antigen generation (Lazaro et al., 2015; Towne et al., 2005), was independent of the length of the peptide, confirming the specialization of ERAP1 for larger peptides (Fig. 3).

3.3. Peptide length selection is affected by SNPs

Using the LG_xL series as a tool to study the length selection properties of ERAP1 we measured the specific activity of N-terminal leucine residue excision by each ERAP1 allele (Fig. S1). While all alleles were able to excise the N-terminus efficiently, the specific activities varied by up to one order of magnitude depending on the allele and peptide studied. More importantly, the overall motif of length degradation was not the same amongst different alleles. For example, the KE allele was less efficient in trimming larger peptides compared to the ancestral KQ allele, but was more efficient in trimming smaller length peptides (Fig. S1).

3.4. Correlation of polymorphic variation and length selection

The observation that ERAP1 alleles exhibit different motifs in trimming a collection of peptides with different lengths, prompted us to analyze this length dependence further. To that end, we normalized the trimming rate of each peptide to the trimming rate of the ancestral ERAP1-KQ. The results were plotted as a function of peptide length allowing us to discern the effect of particular polymorphisms on the length preferences of ERAP1 (Fig. 4). This analysis showed that position 528 does not appear to affect length selection, but rather affects enzyme activity in a uniform manner (panel A, the slope of the correlation is close to 0, but the x-axis intercept is about 0.5, indicating that the RQ variant has about 50% of the activity of the KQ variant). In contrast, the Q730E substitution resulted in a negative slope, indicating that this change leads to an increased preference for smaller peptides (panel B). Interestingly, the combined substitution at positions 528 and 730 resulted to a correlation with a negative slope, as well as a reduced overall activity (as evidenced from the x-axis scale, panel C) suggesting that the two effects (lower activity for all peptides and different length preferences) are independent and additive. The sharp difference in effects between positions 528 and 730 may be rationalized based on the location of these SNPs in the ERAP1 structure. Position 730 lies within the internal cavity of ERAP1 that has been hypothesized to accommodate the peptidic substrates and is in close proximity to a proposed ERAP1 regulatory region (Fig. S2) (Gandhi et al., 2011). It is therefore, possible that SNP at position 730 interferes directly with the ability of longer peptides to bind or to self-activate their own trimming as previously proposed (Nguyen et al., 2011). In particular, polymorphism 730E, carries a negative charge that may affect the local electrostatic potential hindering accommodation of the negatively charged C-terminus of long peptides. In contrast, position 528 is located on the exterior facet of ERAP1, away from the peptide binding cavity and has no possibility to interact directly with the peptide substrate, suggesting that it should be excreting effects on enzymatic activity by a distinct mechanism.

3.5. Molecular dynamics simulations of the three ERAP1 variants

Changes in enzymatic activity due to polymorphic variation at locations within the peptide binding cavity of ERAP1 may be understood in terms of altered interactions with the peptide-substrates. However, the most consistently discovered disease-associated SNP, located at position 528, does not reside within this cavity, but is rather located at the beginning of domain III facing the solvent (Fig. 1). Domain III is a hinge domain that lies in-between of domains II and IV, the two domains that re-orient in respect to each other during the conformational change of the enzyme (Nguyen et al., 2011). Since this conformational change has been proposed to be instrumental to the catalytic cycle of ERAP1, we hypothesized that altered molecular dynamics in domain III may affect the conformational equilibrium of the enzyme and therefore indirectly affect activity.

Please cite this article in press as: Stamogiannos, A., et al., Effects of polymorphic variation on the mechanism of Endoplasmic Reticulum Aminopeptidase 1. Mol. Immunol. (2015), http://dx.doi.org/10.1016/j.molimm.2015.07.010

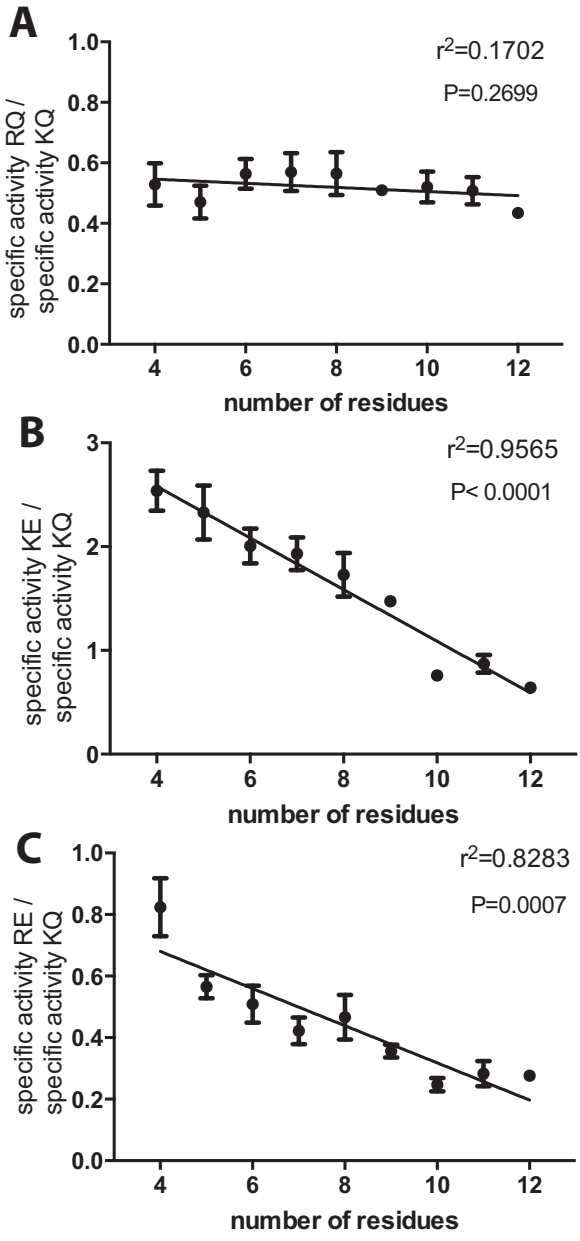

Fig. 4. Trimming rates ratios for different peptide lengths. In each panel the ratio between the specific activity of two ERAP1 variants is plotted versus the length of the peptide substrate. In all cases the denominator is the specific activity of the 528K, 730Q variant (variant KQ). Variant 528R, 730Q (variant RQ) is shown in panel A, variant 528K, 730E (KE) is shown in panel B and variant 528R, 730E (RE) in panel C. The solid line corresponds to a linear regression model. The r^2 value for each regression and the p value for each correlation are also shown.

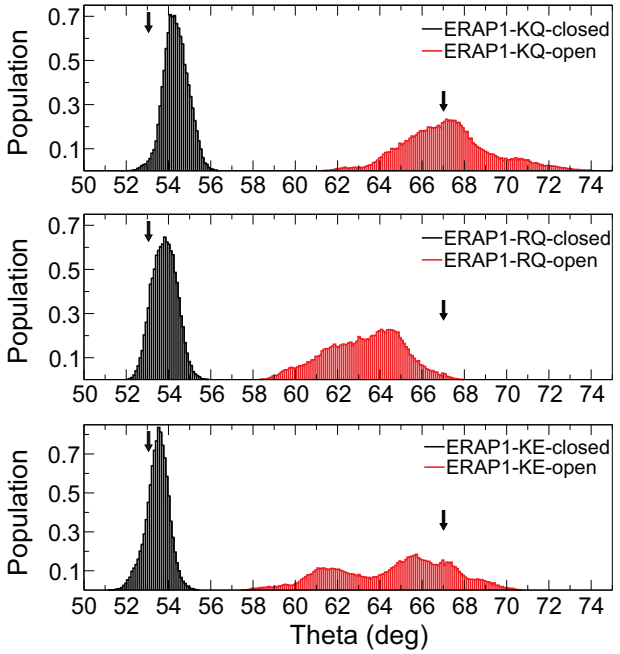

Fig. 5. Normalized histograms of the interdomain angle theta of the three ERAP1 variants acquired from classical MD simulations of 100-ns production runs initialized in the closed (black) and the open (red) states. (For interpretation of the references to color in this figure legend and text, the reader is referred to the web version of this article.)

Conventional molecular dynamics (cMD) of 110 ns were performed for the ERAP1 variants KQ, RQ, and KE in both the open and closed conformations that have been determined by X-ray crystallography. The backbone root-mean-square deviation (RMSD) of simulations initiated in the closed state were stabilized at values of 0.16–0.17 nm, whereas, the open conformations displayed higher flexibility with backbone RMSD values as high as 0.4–0.5 nm (Fig. S3). This was also reflected on the distribution of the interdomain angle theta from the six cMD simulations (Fig. 5). All three ERAP1 variants in the closed state remained closed, while the open conformations sampled a wider range of interdomain angles. This conclusion is consistent with MD simulations for other ligand-free hinge-bending proteins (Pang et al., 2005; Kandt et al., 2006; Shi et al., 2009). In particular, the closed states (Fig. 5, black bars) exhibit a clear-cut maximum around 54°, which corresponds to a slightly more "relaxed" conformation compared to the X-ray structure (53°). The open ERAP1-KQ (Fig. 5, red bars) displayed a fluctuation of interdomain angles between 62 and 72°, with a maximum close to the open X-ray structure at 67°. Interestingly, the open ERAP1-RQ visited more closed states at 59–67°, while ERAP1-KE sampled a wider range of theta between 58 and 70°.

To enhance sampling of the open-closed transition, five independent accelerated molecular dynamics (aMD) simulations were performed on each variant. The key advantage of aMD is that it can effectively explore long timescale motions and large regions of phase space in the absence of a pre-defined reaction coordinate. In previous studies, aMD have been successfully employed in the study of slow timescale dynamics in a variety of proteins (Hamelberg and McCammon, 2005; Markwick et al., 2009; Markwick et al., 2010; Grant et al., 2009; Bucher et al., 2011). Our analysis indicated that for the aMD simulations initialized in closed states, ERAP1 remained closed, even though it did sample a wider range of phase space compared to cMD (Fig. 6). Similarly, the aMD simulations that were seeded from the open ERAP1 resulted to structures that sampled a significantly larger region towards more closed conformations (Supporting information Fig. S4). The open ERAP1-KQ aMD trajectories exhibit a wide range of interdomain angles at 58–72°, which is indicative of small energy barriers between more open and more closed conformations with respect to the X-ray structures. In sharp contrast, most of the open ERAP1-RQ aMD simulations sampled conformations in which theta <60° (Supporting information Fig. S4), resulting in a high-population peak of semi-closed conformations at 57°. The ERAP1-KE variant displayed a broad sampling of conformations between the open and closed states similar to the ancestral ERAP1-KQ, albeit the distribution of the interdomain angle was shifted towards more closed conformations (Fig. 6). Overall, our analysis indicated that the K528R polymorphism has strong effects on the conformational distribu-

Please cite this article in press as: Stamogiannos, A., et al., Effects of polymorphic variation on the mechanism of Endoplasmic Reticulum Aminopeptidase 1. Mol. Immunol. (2015), http://dx.doi.org/10.1016/j.molimm.2015.07.010

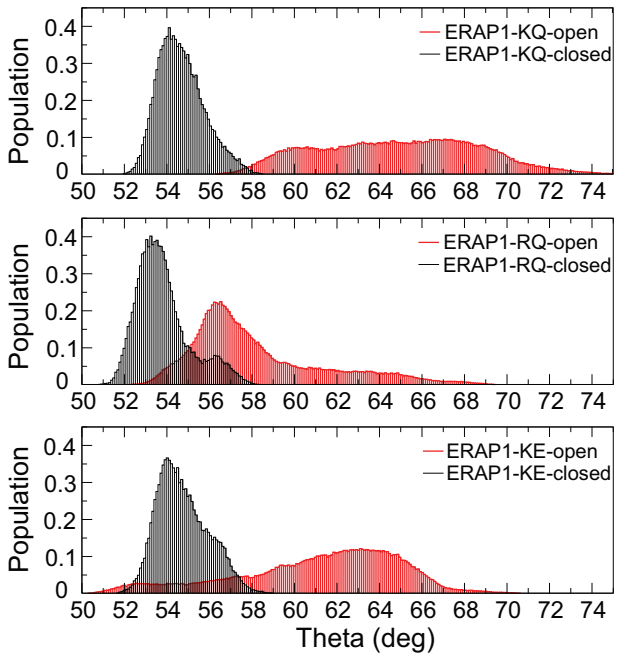

Fig. 6. Normalized histograms of the interdomain angle theta acquired from aMD simulations of the three ERAP1 variants initialized either in the closed (black), or in the open (red) states. (For interpretation of the references to color in this figure legend, the reader is referred to the web version of this article.)

tion of ERAP1 and a limited effect could also be discerned for the Q730E polymorphism.

Principal component analysis (PCA) of the aMD trajectories revealed that motions along the first PCA mode (PC1) describe the open-to-close transition, and along the second mode (PC2) a twist motion primarily between domains I and IV (Fig. 7A). PC1 and PC2 describe, respectively, 46.2% and 18.2% of the total variance of the motions in the aMD simulation of ERAP1-KQ. A two-dimensional representation of the trajectories as a projection of the Boltzmann reweighted distribution onto the PC1–PC2 subspace describes a free energy profile of the three ERAP1 variants (Supporting information Figs. S5–S7). aMD trajectories were reweighted using a Maclaurin series expansion that approximates the exponential Boltzmann factor, which has been shown recently to greatly suppresses the energetic noise (Miao et al., 2014). Comparison of the free energy surfaces obtained from aMD simulations suggests that the K528R polymorphism (RQ variant) induces a conformational shift towards more closed conformations (Fig. 7B). While both the KQ and KE variants sample a wide range of open conformations within 8–10 KJ/mol from the energy minimum, ERAP1-RQ is restricted to a narrower subspace between the open and closed conformations and requires >12 KJ/mol to reach the crystallographic open state. This is mainly attributed to the observation that aMD simulations of ERAP1-RQ spent the majority of the time in an energy basin of a semi-closed conformation (Supporting information Fig. S6). Although this method may suffer from low accuracy in the precise calculation of the energy minima (2–3k_BT) and inherent inaccuracies of the force field (Miao et al., 2014), the relative changes in the energy landscape indicate that, at the very minimum, SNPs in ERAP1 can affect conformational dynamics.

4. Discussion

Molecular components of the human immune system can be highly polymorphic as a result of host-pathogen balancing selection processes and evolutionary pressures. The most prominent example of this is the HLA molecules, which exist as thousands of different allelic forms in the human population and affect both infection susceptibility as well as predisposition to autoimmunity. Being the immediately preceding step in the pathway of antigen presentation, antigen generation by ERAP1 is a potential balancing selection target that modulates infection susceptibility (Cagliani et al., 2010). Not surprisingly, ERAP1 is also polymorphic, with ERAP1 SNPs found to associate with predisposition to viral infections, virally-induced cancer and autoimmune conditions, often in epistasis to particular HLA-alleles (Stratikos and Stern, 2013; Reche and Reinherz, 2003; Evnouchidou et al., 2012).

In this study, we combined experimental and computational approaches to provide evidence that ERAP1 SNPs can exert their effects on enzyme function by at least two independent and complementary mechanisms. We focused our analysis on two key ERAP1 SNPs, located at positions 528 and 730, since they are the two most commonly discovered SNPs in genetic studies and they represent typical examples of SNP locations: one within the internal cavity of ERAP1 and one on the outside. The polymorphic position 730 lies within the extended internal cavity of ERAP1 and although it is 30 Å away from the active site, it may still interact with the C-terminal moiety of a long peptide substrate as previously reported based on crystallographic data (Gandhi et al., 2011). This observation can potentially explain our experimental results: the nature of amino acid at that location may affect recognition of the longer peptide substrates and therefore length selection. In contrast, position 528 is not located inside the internal cavity of ERAP1 and as a result, it is unlikely that it can interact with a peptide substrate. Our computational analysis however, suggests that the nature of amino acid at position 528 of the hinge domain III can indirectly affect enzymatic function by affecting the conformational dynamics of ERAP1. Since any experimentally observed enzymatic activity of ERAP1 includes multiple catalytic cycles and repeated substrate binding and product releases, the conformational plasticity of the enzyme can be expected to affect the apparent enzymatic activity. As a result, variants that are more limited in conformational dynamics may be slower in product release and substrate re-capture, resulting in apparent lower enzymatic activity. Indeed, the variants that carry the 528R polymorphism (RQ and RE) are both found to have lower enzymatic activity compared to the variants that carry the 528K polymorphism (KQ and KE) (Figs. 2 and 4). Some effects on the conformational distribution of ERAP1 can be seen for the polymorphism Q730E and these may driven by subtle changes in the internal cavity electrostatic potential. Overall, our findings provide a mechanistic framework for understanding – and are consistent with – previous observations on cellular models that have suggested independent influences of these two SNPs on the function of ERAP1 and on the length of antigenic peptides generated (Chen et al., 2014; Garcia-Medel et al., 2012; Sanz-Bravo et al., 2015).

Our analysis on length selection, suggested that the Q730E variation may affect length selection by ERAP1, by promoting the trimming of smaller peptides, smaller than 9 amino acids long. Although this may sound counter-intuitive in the context of the role of ERAP1 in antigenic peptide generation, it can be understood in terms of the proposed role of ERAP1 in antigenic peptide destruction by over-trimming (Seregin et al., 2013; York et al., 2002). In addition, the destruction of smaller peptides in the ER may regulate ERAP1 activity by allosteric activation or inhibition (Nguyen et al., 2011; Evnouchidou et al., 2011). Altered trimming of small peptides may also be relevant to other functions of ERAP1 in the context of innate immunity or blood pressure regulation through Angiotensin degradation (Goto et al., 2006; Aldhamen et al., 2015; Hisatsune et al., 2015).

Previous studies have suggested that the peptide-substrate sequence is an important determinant of the trimming rate by ERAP1 and different sequences beyond the N-terminal residue

Please cite this article in press as: Stamogiannos, A., et al., Effects of polymorphic variation on the mechanism of Endoplasmic Reticulum Aminopeptidase 1. Mol. Immunol. (2015), http://dx.doi.org/10.1016/j.molimm.2015.07.010

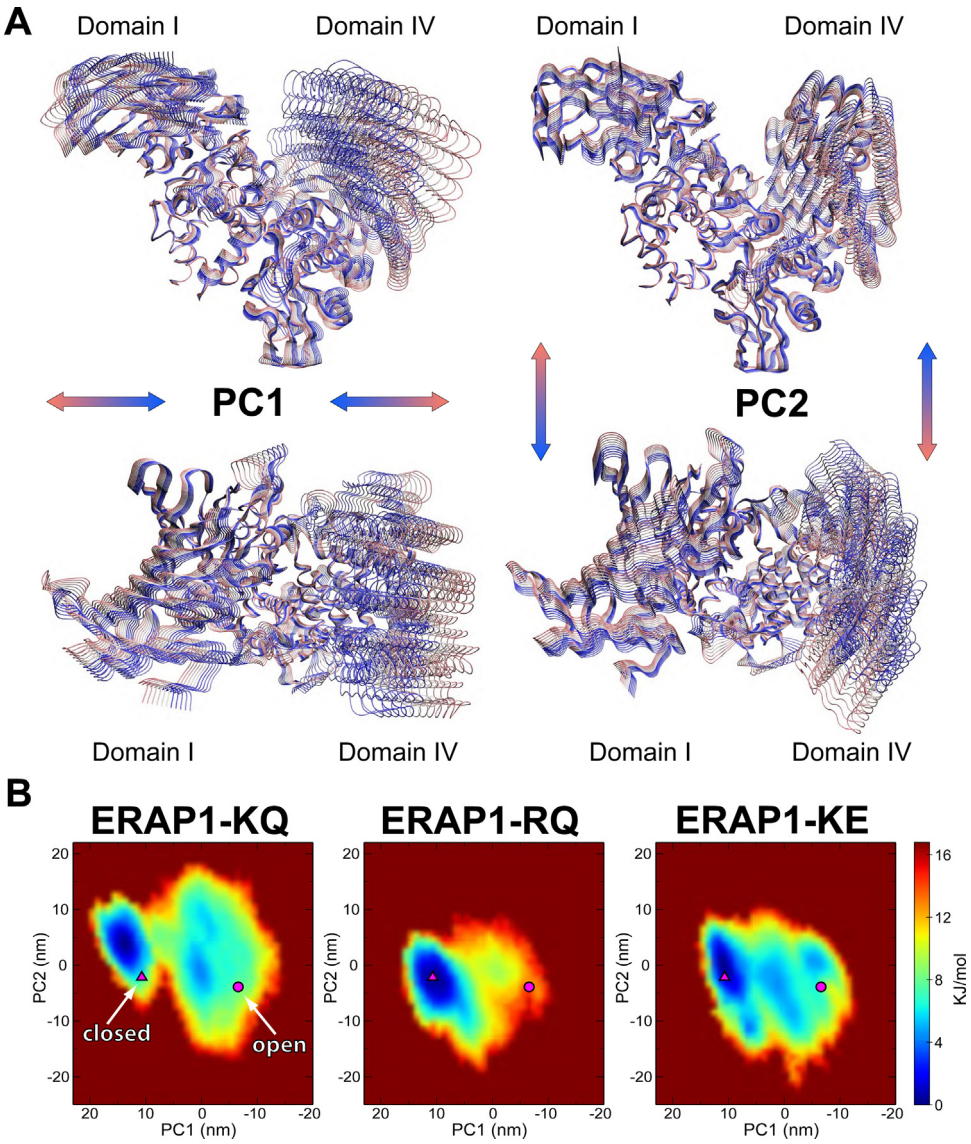

Fig. 7. (A) Motions along the first two principal components (PC1 and PC2) calculated from the aMD trajectories of ERAP1 KQ shown from the side (upper panels) and the top (lower panels) as in Fig. 1. Projections go from positive values in blue to negative ones in red. (B) Free energy principal component projection of the aMD trajectories on the first two principal component vectors (PC1 and PC2) calculated from the ERAP1-KQ aMD trajectory. The PCA plots are reweighted based on a Maclaurin series expansion to the 10th order, and the crystallographic structures of the closed (triangle) and open (circle) ERAP1 states are projected onto the free energy surface. (For interpretation of the references to color in this figure legend, the reader is referred to the web version of this article.)

can affect processing rates by several orders of magnitude (Chang et al., 2005; Evnouchidou et al., 2008; Evnouchidou et al., 2011; Georgiadou et al., 2010). In addition, polymorphic variation at positions 528 and 730 was shown to affect processing of different sequences in complex patterns suggesting that peptide-substrate recognition may be influenced by polymorphic variation (Evnouchidou et al., 2011). The mechanisms we describe in this study are, at first approximation, sequence-independent and may be complementary to sequence-dependent effects in shaping the immunopeptidome, although the extent of that contribution is unclear. Although for particular epitopes, the sequence may be a major determinant, in the context of the sum of peptides processed by ERAP1, sequence-dependent effects may be smoothed and sequence-independent effects, like length selection and conformational plasticity may be easier to observe (Chen et al., 2014; Garcia-Medel et al., 2012; Sanz-Bravo et al., 2015).

The discovery that ERAP1 exists in at least two largely different conformations, one of which allows no external access to the catalytic site has led researchers to propose a two-step mechanism for peptide trimming: initial capture of the peptide by the open-state leads to a large conformational rearrangement that optimizes the orientation of key catalytic residues and residues in the S1 pocket of the enzyme to promote catalysis (Nguyen et al., 2011; Kochan et al., 2011). Our MD analysis indicates the pre-existence of equilibrium dynamics that promote the sampling of multiple open states. This finding is consistent with a two-step mechanism of ligand recognition. Such a mechanism is also consistent with the biological function of ERAP1 that includes trimming of peptides of different lengths, whose initial capture is facilitated by open conformational states. The wide-distribution of open states revealed by the MD calculations suggests a relatively flat free-energy pathway linking several conformations of similar free energies (Bucher et al., 2011). Even minor amino acid substitutions throughout the protein structure can affect the sampling of this pathway, leading to changes in conformational distribution and changes to apparent enzymatic activity. This mechanism can lead to the evolutionary advantage of being able to fine-tune the activity of the enzyme by multiple polymorphic substitutions away from the active site.

Please cite this article in press as: Stamogiannos, A., et al., Effects of polymorphic variation on the mechanism of Endoplasmic Reticulum Aminopeptidase 1. Mol. Immunol. (2015), http://dx.doi.org/10.1016/j.molimm.2015.07.010

Our results provide an operational framework for understanding the effects of ERAP1 SNPs on enzyme function: (i) SNPs that lie within the internal cavity of ERAP1 may influence substrate binding, or product release—their effects will depend on their exact location (and distance from the catalytic site) and the length and nature of the substrate, (ii) SNPs that lie in the hinge domain III of ERAP1 may exert their effects indirectly by influencing the conformational plasticity of the enzyme and the rate of completion of each catalytic cycle. These two mechanisms can be independent and complementary to each other, as suggested by our data. It is possible however, that SNPs within the internal cavity of ERAP1 can also affect conformational dynamics indirectly by changing the on/off rate of substrate capture. To date, no ERAP1-peptide substrate crystal structure exists to allow the computational modeling of this idea.

The ability to regulate ERAP1 activity by random mutations at many functional domains of the enzyme may be highly beneficial for maintaining variability in adaptive immune responses, and for rapid adaptations depending on interaction with novel pathogens. Mutations away from the active site should be much easier to tolerate since they should not lead to completely inactive enzyme. Sampling different locations for variation allows the immune system to generate an array of different ERAP1 activities that we now know they can affect immunodominance and responses to disease (Alvarez-Navarro and Lopez de Castro, 2014; Reeves et al., 2013; Sanz-Bravo et al., 2015; Alvarez-Navarro et al., 2015). Indeed, recent work has been slowly revealing that ERAP1 samples a highly dynamic range of activities in different individuals, from hyper-trimming to hypo-trimming, affecting adaptive immune responses (Reeves et al., 2014). This may be difficult to achieve by mutations within the active site that often have major effects on activity. Instead, modulating ERAP1 activity by distant mutations that result in small effects may constitute an effective approach to testing immune response variations without risk of shutting down key pathways. It is slowly becoming apparent that ERAP1 SNPs will play key roles both in promoting our understanding of disease predisposition, but also in developing new therapies that rely on the pharmaceutical modulation of ERAP1 activity (Zervoudi et al., 2013; Papakyriakou et al., 2015; Stratikos, 2014).

Author contributions

A.S. analyzed experimental data, prepared the recombinant enzymes, purified the peptides and performed the enzymatic assays. D.K. performed enzymatic assays and analyzed data. A.P. conceived, designed and executed the computational analysis. E.S. conceived, supervised the project and analyzed data. All authors contributed to the preparation of the manuscript and have approved its final version.

Acknowledgements

This research was financed by the European Union (European Social Fund) and Greek national funds through the Operational Program “Education and Lifelong Learning” of the National Strategic Reference Framework: Research Funding Program of the General Secretariat for Research & Technology (Grant ERC-14).

Appendix A. Supplementary data

Supplementary data associated with this article can be found, in the online version, at http://dx.doi.org/10.1016/j.molimm.2015.07.010

References

Aldhamen, Y.A., Pepelyayeva, Y., Rastall, D.P., Seregin, S.S., Zervoudi, E., Koumantou, D., Aylsworth, C.F., Quiroga, D., Godbehere, S., Georgiadis, D., Stratikos, E., Amalfitano, A., 2015. Autoimmune disease-associated variants of extracellular endoplasmic reticulum aminopeptidase 1 induce altered innate immune responses by human immune cells. J. Innate Immun. 7, 275–289.

Alvarez-Navarro, C., Lopez de Castro, J.A., 2014. ERAP1 structure, function and pathogenetic role in ankylosing spondylitis and other MHC-associated diseases. Mol. Immunol. 57, 12–21.

Alvarez-Navarro, C., Martin-Esteban, E., Admon, A., Lopez de Castro, J.A., 2015. ERAP1 polymorphism relevant to inflammatory disease shapes the peptidome of the birdshot chorioretinopathy-associated HLA-A *29:02 antigen. Mol. Cell Proteomics 14, 1770–1780.

Anandakrishnan, R., Aguilar, B., Onufriev, A.V., 2012. H++ 3.0: automating pK prediction and the preparation of biomolecular structures for atomistic molecular modeling and simulations. Nucleic Acids Res. 40, W537–W541.

Berendsen, H.J.C., Postma, J.P.M., Vangunsteren, W.F., Dinola, A., Haak, J.R., 1984. Molecular-dynamics with coupling to an external bath. J. Chem. Phys. 81, 3684–3690.

Blanchard, N., Shastri, N., 2008. Coping with loss of perfection in the MHC class I peptide repertoire. Curr. Opin. Immunol. 20, 82–88.

Bucher, D., Grant, B.J., Markwick, P.R., McCammon, J.A., 2011. Accessing a hidden conformation of the maltose binding protein using accelerated molecular dynamics. PLoS Comput. Biol. 7 (4), e1002034.

Cagliani, R., Riva, S., Biasin, M., Fumagalli, M., Pozzoli, U., Lo Caputo, S., Mazzotta, F., Piacentini, L., Bresolin, N., Clerici, M., Sironi, M., 2010. Genetic diversity at endoplasmic reticulum aminopeptidases is maintained by balancing selection and is associated with natural resistance to HIV-1 infection. Hum. Mol. Genet. 19, 4705–4714.

Case, D.A., Cheatham, T.E., Darden, T., Gohlke, H., Luo, R., Merz, K.M., Onufriev, A., Simmerling, C., Wang, B., Woods, R.J., 2005. The Amber biomolecular simulation programs. J. Comput. Chem. 26, 1668–1688.

Chang, S.C., Momburg, F., Bhutani, N., Goldberg, A.L., 2005. The ER aminopeptidase, ERAP1, trims precursors to lengths of MHC class I peptides by a molecular ruler mechanism. Proc. Natl. Acad. Sci. U. S. A. 102, 17107–17112.

Chen, L., Fischer, R., Peng, Y., Reeves, E., McHugh, K., Ternette, N., Hanke, T., Dong, T., Elliott, T., Shastri, N., Kollnberger, S., James, E., Kessler, B., Bowness, P., 2014. Critical Role of Endoplasmic Reticulum Aminopeptidase 1 in Determining the Length and Sequence of Peptides Bound and Presented by HLA-B27. Arthritis & rheumatology (Hoboken, N.J.) 66, 284–294.

Darden, T., York, D., Pedersen, L., 1993. Particle mesh Ewald – an *N*. Log(*N*) method for Ewald sums in large systems. J. Chem. Phys. 98, 10089–10092.

Evans, D.M., Spencer, C.C., Pointon, J.J., Su, Z., Harvey, D., Kochan, G., Oppermann, U., Dilthey, A., Pirinen, M., Stone, M.A., Appleton, L., Moutsianas, L., Leslie, S., Wordsworth, T., Kenna, T.J., Karaderi, T., Thomas, G.P., Ward, M.M., Weisman, M.H., Farrar, C., Bradbury, L.A., Danoy, P., Inman, R.D., Maksymowych, W., Gladman, D., Rahman, P., Spondyloarthritis Research Consortium of, C., Morgan, A., Marzo-Ortega, H., Bowness, P., Gaffney, K., Gaston, J.S., Smith, M., Bruges-Armas, J., Couto, A.R., Sorrentino, R., Paladini, F., Ferreira, M.A., Xu, H., Liu, Y., Jiang, L., Lopez-Larrea, C., Diaz-Pena, R., Lopez-Vazquez, A., Zayats, T., Band, G., Bellenguez, C., Blackburn, H., Blackwell, J.M., Bramon, E., Bumpstead, S.J., Casas, J.P., Corvin, A., Craddock, N., Deloukas, P., Dronov, S., Duncanson, A., Edkins, S., Freeman, C., Gillman, M., Gray, E., Gwilliam, R., Hammond, N., Hunt, S.E., Jankowski, J., Jayakumar, A., Langford, C., Liddle, J., Markus, H.S., Mathew, C.G., McCann, O.T., McCarthy, M.I., Palmer, C.N., Peltonen, L., Plomin, R., Potter, S.C., Rautanen, A., Ravindrarajah, R., Ricketts, M., Samani, N., Sawcer, S.J., Strange, A., Trembath, R.C., Viswanathan, A.C., Waller, M., Weston, P., Whittaker, P., Widaa, S., Wood, N.W., McVean, G., Reveille, J.D., Wordsworth, B.P., Brown, M.A., Donnelly, P., Australo-Anglo-American Spondyloarthritis, C., Wellcome Trust Case Control, C., 2011. Interaction between ERAP1 and HLA-B27 in ankylosing spondylitis implicates peptide handling in the mechanism for HLA-B27 in disease susceptibility. Nat. Genet. 43, 761–767.

Evnouchidou, I., Momburg, F., Papakyriakou, A., Chroni, A., Leondiadis, L., Chang, S.C., Goldberg, A.L., Stratikos, E., 2008. The internal sequence of the peptide-substrate determines its N-terminus trimming by ERAP1. PLoS One 3, e3658.

Evnouchidou, I., Papakyriakou, A., Stratikos, E., 2009. A new role for Zn(II) aminopeptidases: antigenic peptide generation and destruction. Curr. Pharm. Design 15, 3656–3670.

Evnouchidou, I., Kamal, R.P., Seregin, S.S., Goto, Y., Tsujimoto, M., Hattori, A., Voulgari, P.V., Drosos, A.A., Amalfitano, A., York, I.A., Stratikos, E., 2011. Coding single nucleotide polymorphisms of endoplasmic reticulum aminopeptidase 1 can affect antigenic peptide generation in vitro by influencing basic enzymatic properties of the enzyme. J. Immunol. 186, 1909–1913.

Evnouchidou, I., Birtley, J., Seregin, S., Papakyriakou, A., Zervoudi, E., Samiotaki, M., Panayotou, G., Giastas, P., Petrakis, O., Georgiadis, D., Amalfitano, A., Saridakis, E., Mavridis, I.M., Stratikos, E., 2012. A common single nucleotide polymorphism in endoplasmic reticulum aminopeptidase 2 induces a specificity switch that leads to altered antigen processing. J. Immunol. 189, 2383–2392.

Fiser, A., Sali, A., 2003. MODELLER: generation and refinement of homology-based protein structure models. Macromol. Crystallogr. 374, 461–491.

Fruci, D., Romania, P., D'Alicandro, V., Locatelli, F., 2014. Endoplasmic reticulum aminopeptidase 1 function and its pathogenic role in regulating innate and

adaptive immunity in cancer and major histocompatibility complex class I-associated autoimmune diseases. Tissue Antigens 84, 177–186.
Gandhi, A., Lakshminarasimhan, D., Sun, Y., Guo, H.C., 2011. Structural insights into the molecular ruler mechanism of the endoplasmic reticulum aminopeptidase ERAP1. Sci. Rep. 1, 186.
Garcia-Medel, N., Sanz-Bravo, A., Van Nguyen, D., Galocha, B., Gomez-Molina, P., Martin-Esteban, A., Alvarez-Navarro, C., de Castro, J.A., 2012. Functional interaction of the ankylosing spondylitis-associated endoplasmic reticulum aminopeptidase 1 polymorphism and HLA-B27 in vivo. Mol. Cell Proteomics 11, 1416–1429.
Georgiadou, D., Hearn, A., Evnouchidou, I., Chroni, A., Leondiadis, L., York, I.A., Rock, K.L., Stratikos, E., 2010. Placental leucine aminopeptidase efficiently generates mature antigenic peptides in vitro but in patterns distinct from endoplasmic reticulum aminopeptidase 1. J. Immunol. 185, 1584–1592.
Goto, Y., Hattori, A., Ishii, Y., Tsujimoto, M., 2006. Reduced activity of the hypertension-associated Lys528Arg mutant of human adipocyte-derived leucine aminopeptidase (A-LAP)/ER-aminopeptidase-1. FEBS Lett. 580, 1833–1838.
Grant, B.J., Gorfe, A.A., McCammon, J.A., 2009. Ras conformational switching: simulating nucleotide-dependent conformational transitions with accelerated molecular dynamics. PLoS Comput. Biol. 3, e1000325.
Hamelberg, D., McCammon, J.A., 2005. Fast peptidyl cis–trans isomerization within the flexible Gly-rich flaps of HIV-1 protease. J. Am. Chem. Soc. 127, 13778–13779.
Hamelberg, D., Mongan, J., McCammon, J.A., 2004. Accelerated molecular dynamics: a promising and efficient simulation method for biomolecules. J. Chem. Phys. 120, 11919–11929.
Hamelberg, D., de Oliveira, C.A.F., McCammon, J.A., 2007. Sampling of slow diffusive conformational transitions with accelerated molecular dynamics. J. Chem. Phys. 127, 155102.
Hisatsune, C., Ebisui, E., Usui, M., Ogawa, N., Suzuki, A., Mataga, N., Takahashi-Iwanaga, H., Mikoshiba, K., 2015. ERp44 exerts redox-dependent control of blood pressure at the ER. Mol. Cell 58, 1015–1027.
Hornak, V., Abel, R., Okur, A., Strockbine, B., Roitberg, A., Simmerling, C., 2006. Comparison of multiple Amber force fields and development of improved protein backbone parameters. Proteins 65, 712–725.
Humphrey, W., Dalke, A., Schulten, K., 1996. VMD: visual molecular dynamics. J. Mol. Graph Model 14, 33–38.
Jorgensen, W.L., Chandrasekhar, J., Madura, J.D., Impey, R.W., Klein, M.L., 1983. Comparison of simple potential functions for simulating liquid water. J. Chem. Phys. 79, 926–935.
Kandt, C., Xu, Z.T., Tieleman, D.P., 2006. Opening and closing motions in the periplasmic vitamin B-12 binding protein BtuF. Biochemistry 45, 13284–13292.
Kochan, G., Krojer, T., Harvey, D., Fischer, R., Chen, L., Vollmar, M., von Delft, F., Kavanagh, K.L., Brown, M.A., Bowness, P., Wordsworth, P., Kessler, B.M., Oppermann, U., 2011. Crystal structures of the endoplasmic reticulum aminopeptidase-1 (ERAP1) reveal the molecular basis for N-terminal peptide trimming. Proc. Natl. Acad. Sci. U. S. A. 108, 7745–7750.
Lazaro, S., Gamarra, D., Del Val, M., 2015. Proteolytic enzymes involved in MHC class I antigen processing: a guerrilla army that partners with the proteasome. Mol. Immunol., http://dx.doi.org/10.1016/j.molimm.2015.04.014
Markwick, P.R.L., Bouvignies, G., Salmon, L., McCammon, J.A., Nilges, M., Blackledge, M., 2009. Toward a unified representation of protein structural dynamics in solution. J. Am. Chem. Soc. 131, 16968–16975.
Markwick, P.R.L., Cervantes, C.F., Abel, B.L., Komives, E.A., Blackledge, M., McCammon, J.A., 2010. Enhanced conformational space sampling improves the prediction of chemical shifts in proteins. J. Am. Chem. Soc. 132, 1220–1221.
Martin-Esteban, A., Gomez-Molina, P., Sanz-Bravo, A., Lopez de Castro, J.A., 2014. Combined effects of ankylosing spondylitis-associated ERAP1 polymorphisms outside the catalytic and peptide-binding sites on the processing of natural HLA-B27 ligands. J. Biol. Chem. 289, 3978–3990.
Miao, Y.L., Sinko, W., Pierce, L., Bucher, D., Walker, R.C., McCammon, J.A., 2014. Improved reweighting of accelerated molecular dynamics simulations for free energy calculation. J. Chem. Theory Comput. 10, 2677–2689.
Nguyen, T.T., Chang, S.C., Evnouchidou, I., York, I.A., Zikos, C., Rock, K.L., Goldberg, A.L., Stratikos, E., Stern, L.J., 2011. Structural basis for antigenic peptide precursor processing by the endoplasmic reticulum aminopeptidase ERAP1. Nat. Struct. Mol. Biol. 18, 604–613.
Pang, A., Arinaminpathy, Y., Sansom, M.S.P., Biggin, P.C., 2005. Comparative molecular dynamics – similar folds and similar motions? Proteins-Struct. Funct. Bioinf. 61, 809–822.
Papakyriakou, A., Spyroulias, G.A., Sturrock, E.D., Manessi-Zoupa, E., Cordopatis, P., 2007. Simulated interactions between angiotensin-converting enzyme and substrate gonadotropin-releasing hormone: novel insights into domain selectivity. Biochemistry 46, 8753–8765.
Papakyriakou, A., Zervoudi, E., Tsoukalidou, S., Mauvais, F.X., Sfyroera, G., Mastellos, D.C., van Endert, P., Theodorakis, E.A., Vourloumis, D., Stratikos, E., 2015. 3,4-Diaminobenzoic acid derivatives as inhibitors of the oxytocinase subfamily of M1 aminopeptidases with immune-regulating properties. J. Med. Chem. 58, 1524–1543.
Pastor, R.W., Brooks, B.R., Szabo, A., 1988. An analysis of the accuracy of langevin and molecular-dynamics algorithms. Mol. Phys. 65, 1409–1419.
Reche, P.A., Reinherz, E.L., 2003. Sequence variability analysis of human class I and class II MHC molecules: functional and structural correlates of amino acid polymorphisms. J. Mol. Biol. 331, 623–641.
Reeves, E., Edwards, C.J., Elliott, T., James, E., 2013. Naturally occurring ERAP1 haplotypes encode functionally distinct alleles with fine substrate specificity. J. Immunol. 191, 35–43.
Reeves, E., Colebatch-Bourn, A., Elliott, T., Edwards, C.J., James, E., 2014. Functionally distinct ERAP1 allotype combinations distinguish individuals with ankylosing spondylitis. Proc. Natl. Acad. Sci. U. S. A. 111, 17594–17599.
Roe, D.R., Cheatham, T.E., 2013. PTRAJ and CPPTRAJ: software for processing and analysis of molecular dynamics trajectory data. J. Chem. Theory Comput. 9, 3084–3095.
Ryckaert, J.P., Ciccotti, G., Berendsen, H.J.C., 1977. Numerical-integration of cartesian equations of motion of a system with constraints – molecular-dynamics of *N*-alkanes. J. Comput. Phys. 23, 327–341.
Salomon-Ferrer, R., Gotz, A.W., Poole, D., Le Grand, S., Walker, R.C., 2013. Routine microsecond molecular dynamics simulations with AMBER on GPUs.2. explicit solvent particle mesh Ewald. J. Chem. Theory Comput. 9, 3878–3888.
Sanz-Bravo, A., Campos, J., Mazariegos, M.S., Lopez de Castro, J.A., 2015. Dominant Role of the ERAP1 Polymorphism R528K in Shaping the HLA-B27 Peptidome Through Differential Processing Determined by Multiple Peptide Residues. Arthritis & rheumatology (Hoboken, N.J.) 67, 692–701.
Seregin, S.S., Rastall, D.P., Evnouchidou, I., Aylsworth, C.F., Quiroga, D., Kamal, R.P., Godbehere-Roosa, S., Blum, C.F., York, I.A., Stratikos, E., Amalfitano, A., 2013. Endoplasmic reticulum aminopeptidase-1 alleles associated with increased risk of ankylosing spondylitis reduce HLA-B27 mediated presentation of multiple antigens. Autoimmunity 46, 497–508.
Shen, M.Y., Sali, A., 2006. Statistical potential for assessment and prediction of protein structures. Protein Sci. 15, 2507–2524.
Shi, R., Proteau, A., Wagner, J., Cui, Q.Z., Purisima, E.O., Matte, A., Cygler, M., 2009. Trapping open and closed forms of FitE-A group III periplasmic binding protein. Proteins-Struct. Funct. Bioinf. 75, 598–609.
Stratikos, E., Stern, L.J., 2013. Antigenic peptide trimming by ER aminopeptidases-insights from structural studies. Mol. Immunol. 55, 212–219.
Stratikos, E., 2014. Regulating adaptive immune responses using small molecule modulators of aminopeptidases that process antigenic peptides. Curr. Opin. Chem. Biol. 23C, 1–7.
The Australo-Anglo-American Spondyloarthritis, C., the Wellcome Trust Case Control, C., Evans, D.M., Spencer, C.C., Pointon, J.J., Su, Z., Harvey, D., Kochan, G., Opperman, U., Dilthey, A., Pirinen, M., Stone, M.A., Appleton, L., Moutsianis, L., Leslie, S., Wordsworth, T., Kenna, T.J., Karaderi, T., Thomas, G.P., Ward, M.M., Weisman, M.H., Farrar, C., Bradbury, L.A., Danoy, P., Inman, R.D., Maksymowych, W., Gladman, D., Rahman, P., Spondyloarthritis Research Consortium of, C., Morgan, A., Marzo-Ortega, H., Bowness, P., Gaffney, K., Gaston, J.S., Smith, M., Bruges-Armas, J., Couto, A.R., Sorrentino, R., Paladini, F., Ferreira, M.A., Xu, H., Liu, Y., Jiang, L., Lopez-Larrea, C., Diaz-Pena, R., Lopez-Vazquez, A., Zayats, T., Band, G., Bellenguez, C., Blackburn, H., Blackwell, J.M., Bramon, E., Bumpstead, S.J., Casas, J.P., Corvin, A., Craddock, N., Deloukas, P., Dronov, S., Duncanson, A., Edkins, S., Freeman, C., Gillman, M., Gray, E., Gwilliam, R., Hammond, N., Hunt, S.E., Jankowski, J., Jayakumar, A., Langford, C., Liddle, J., Markus, H.S., Mathew, C.G., McCann, O.T., McCarthy, M.I., Palmer, C.N., Peltonen, L., Plomin, R., Potter, S.C., Rautanen, A., Ravindrarajah, R., Ricketts, M., Samani, N., Sawcer, S.J., Strange, A., Trembath, R.C., Viswanathan, A.C., Waller, M., Weston, P., Whittaker, P., Widaa, S., Wood, N.W., McVean, G., Reveille, J.D., Wordsworth, B.P., Brown, M.A., Donnelly, P., 2011. Interaction between ERAP1 and HLA-B27 in ankylosing spondylitis implicates peptide handling in the mechanism for HLA-B27 in disease susceptibility. Nat. Genet. 43, 761–767.
Towne, C.F., York, I.A., Neijssen, J., Karow, M.L., Murphy, A.J., Valenzuela, D.M., Yancopoulos, G.D., Neefjes, J.J., Rock, K.L., 2005. Leucine aminopeptidase is not essential for trimming peptides in the cytosol or generating epitopes for MHC class I antigen presentation. J. Immunol. 175, 6605–6614.
Weimershaus, M., Evnouchidou, I., Saveanu, L., van Endert, P., 2013. Peptidases trimming MHC class I ligands. Curr. Opin. Immunol. 25, 90–96.
York, I.A., Chang, S.C., Saric, T., Keys, J.A., Favreau, J.M., Goldberg, A.L., Rock, K.L., 2002. The ER aminopeptidase ERAP1 enhances or limits antigen presentation by trimming epitopes to 8-9 residues. Nat. Immunol. 3, 1177–1184.
Zervoudi, E., Saridakis, E., Birtley, J.R., Seregin, S.S., Reeves, E., Kokkala, P., Aldhamen, Y.A., Amalfitano, A., Mavridis, I.M., James, E., Georgiadis, D., Stratikos, E., 2013. Rationally designed inhibitor targeting antigen-trimming aminopeptidases enhances antigen presentation and cytotoxic T-cell responses. Proc. Natl. Acad. Sci. U. S. A. 110, 19890–19895.

Please cite this article in press as: Stamogiannos, A., et al., Effects of polymorphic variation on the mechanism of Endoplasmic Reticulum Aminopeptidase 1. Mol. Immunol. (2015), http://dx.doi.org/10.1016/j.molimm.2015.07.010